Cross-sensor radiometric normalization of Planet smallsat data using Sentinel-2 to improve consistency across scenes and environments

Hemingway, Benjamin, Frazier, Amy

Benjamin L. Hemingway, Amy E. Frazier, "Cross-sensor radiometric normalization of Planet smallsat data using Sentinel-2 to improve consistency across scenes and environments," Proc. SPIE 11862, Image and Signal Processing for Remote Sensing XXVII, 1186204 (12 September 2021); doi: 10.1117/12.2600246

SPIE.

Event: SPIE Remote Sensing, 2021, Online Only

Cross-sensor radiometric normalization of Planet smallsat data using Sentinel-2 to improve consistency across scenes and environments

Benjamin L. Hemingway*[a], Amy E. Frazier[a]
[a]School of Geographical Sciences and Urban Planning, Arizona State University, 975 S. Myrtle Ave. Tempe, AZ, USA 85281

ABSTRACT

Commercial smallsats are emerging as a key resource for the remote sensing community, with Planet Labs, Inc. operating the largest constellation. Global coverage is achieved through the combined efforts of many different sensors, but the unique spectral response of each sensor results in radiometric inconsistencies across the constellation. These inconsistencies have been an obstacle for researchers as the images do not match the quality the remote sensing community has come to expect from traditional platforms such as Landsat or Sentinel. Various approaches have been offered to correct cross-sensor radiometric inconsistencies in Planet image acquisitions, with many utilizing high radiometric quality platforms such as Landsat or Sentinel to normalize Planet surface reflectance via a linear transformation. These approaches have largely been applied in homogenous regions, and performance in heterogeneous landscapes is not well understood. The Planet surface reflectance images were transformed linearly using Sentinel-2 surface reflectance as a reference. Transformations were tested in six heterogeneous National Ecological Observatory Network sites where airborne hyperspectral data was available for validation. The probability density functions of the transformed Planet images and the corresponding Sentinel reference images were compared using the *D* statistic of the Kolmogorov-Smirnov test. The absolute spectral accuracy of the transformed Planet images was evaluated against airborne hyperspectral data. Results show that the transformations were effective in transforming the empirical cumulative distribution functions of the Planet images to be more similar to that of Sentinel regardless of initial offsets.

Keywords: cubesat; constellation; remote sensing; radiometric correction; signal processing

1. INTRODUCTION

There is a persistent need in the remote sensing community for imaging sensors capable of both very high spatial and temporal resolutions. Commercial small satellites (smallsats or cubestats) are emerging as a key resource for Earth observation. Smallsats are poised to revolutionize Earth observation, augmenting traditional space-based imaging platforms either through filling spatio-temporal gaps or synergistically through data fusion pipelines.

Planet (Planet Labs, Inc) operates the largest constellation of Earth imaging smallsats (called Doves) with more than 180 Doves currently in the constellation. Their small size (10 x 10 x 30 cm) allows them to be built rapidly and inexpensively. Multiple Doves (called Flocks) are able to be delivered into orbit aboard launch vehicles as secondary payloads[1] as Planet's sensor technology advances. Since 2016, Planet has developed and launched three generations of its PlanetScope (PS) sensors, each capable of daily (or near-daily) imaging of Earth at 3-4 m spatial resolution in the RGB + NIR wavebands.

While Planet's PS data are available as orthorectified and atmospherically corrected, there are a number of factors influencing the radiometric consistency that need to be addressed to achieve the performance, reliability, and cross-sensor consistency associated with higher quality, single-source satellite missions such as Landsat or Sentinel[2]. Spatially adjacent scenes may be captured at different times of day and with different sensors, resulting in different illumination characteristics, surface reflectance anisotropy, and sensor response[3]. Such radiometric inconsistencies are particularly apparent when creating multi-image mosaics or time series, requiring additional preprocessing before the images are ready for quantitative scientific analysis.

blheming@asu.edu; phone 1 480 965-7533; fax 1 480 965-8313; sgsup.asu.edu

Image and Signal Processing for Remote Sensing XXVII, edited by Lorenzo Bruzzone, Francesca Bovolo, Proc. of SPIE Vol. 11862, 1186204 · © 2021 SPIE
CCC code: 0277-786X/21/$21 · doi: 10.1117/12.2600246

Radiometric inconsistencies with multi-sensor/multi-temporal data have historically been overcome through radiometric normalization. Radiometric normalization is the process through which radiometric differences related to image acquisition characteristics are empirically reduced[4] by transforming a subject image to match a reference image or a single image in a time series[5]. Often normalization models are trained using spectrally invariant pixels, known as pseudo invariant features (PIF) prior to change detection[6], but such methods are not ideal when change in vegetation phenology is the purpose of the analysis and transformations utilizing all pixels are preferable[4].

Radiometric normalization using a lower resolution but higher radiometric quality reference image (e.g., Sentinel, Landsat) is a cross-sensor calibration method that does not depend on the selection of PIFs[3]. This type of radiometric normalization method has been applied to Planet scenes, with researchers often applying a linear transformation utilizing a coincident Landsat scene[7,8,9]. However, the efficacy of these types of radiometric transformations is not well understood, particularly in heterogeneous terrain[2,10].

The objective of this study is to test the radiometric normalization of PlanetScope imagery across six sites of various heterogeneity using Sentinel as a reference image. A linear transformation is applied to the PS images based on the reference images captured on the same date. The probability density functions of the transformed Planet images and the corresponding Sentinel reference images are compared using the *D* statistic of the Kolmogorov-Smirnoff test. The absolute error associated with transformed Planet images is measured relative to airborne hyperspectral data.

2. STUDY LOCATIONS AND DATA

2.1 Study Locations

Imagery for this study was collected at six National Ecological Observatory Network (NEON) sites in the United States (Fig. 1). NEON is a continental-scale research platform that captures long-term data on land cover change. NEON sites were selected for this study due to the availability if airborne hyperspectral data to be used as a spectral reference. The sites used in this study include Central Plains Experimental Range (CPER), Konza Prairie Biological Station (KONZ), Niwot Ridge (NIWO), University of Notre Dame Environmental Research Center (UNDE), Chase Lake National Wildlife Refuge (WOOD), and Yellowstone National Park (YELL). The geographic coordinates, mean elevations, and dominant National Land Cover Database (NLCD) classification for each site are listed in Table 1.

Table 1. Geographic information about the NEON study sites.

Site	Coordinates	Mean Elevation	Landcover
CPER	40.815536, -104.74559	1,654 m	Grassland/Herbaceous
KONZ	39.100774, -96.563075	414 m	Deciduous Forest, Grassland/Herbaceous
NIWO	40.05425, -105.58237	3,490 m	Evergreen Forest, Grassland/Herbaceous
UNDE	46.23391, -89.537254	521 m	Deciduous Forest, Mixed Forest, Woody Wetlands
WOOD	47.1282, -99.241334	591 m	Emergent Herbaceous Wetlands, Grassland/Herbaceous
YELL	44.95348, -110.53914	2,133 m	Evergreen Forest, Grassland/Herbaceous, Shrub/Scrub

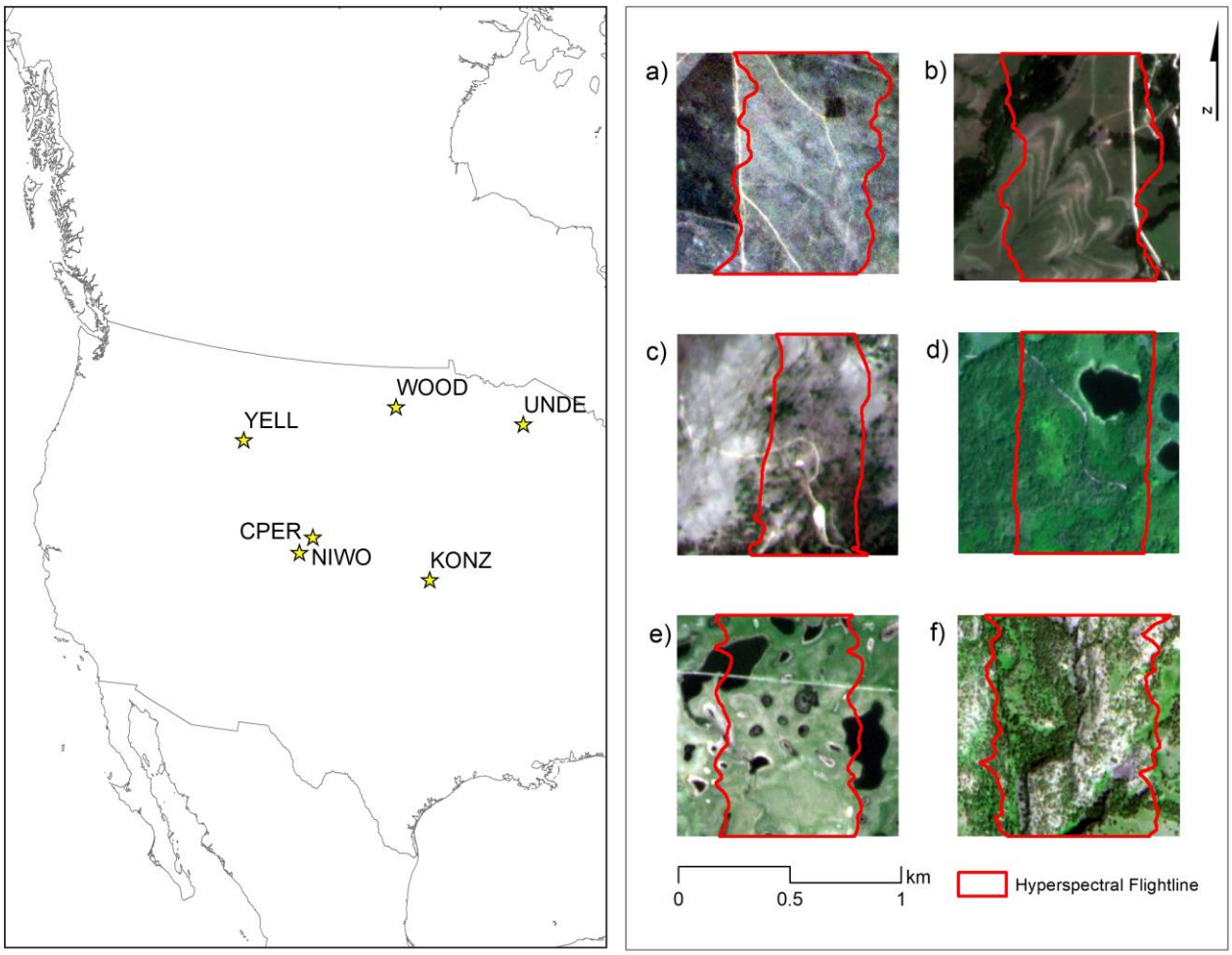

Figure 1. The geographic locations of the six National Ecological Observatory Network (NEON) sites, 1 sq km Planet imagery samples, and NEON hyperspectral flight line boundaries (red boxes) for (a) CPER, (b) KONZ, (c) NIWO, (d) UNDE, (e) WOOD, and (f) YELL.

2.2 Planet and Sentinel Data

Planet scenes were acquired for the six NEON sites for the date closest available to the hyperspectral data acquisition (Table 2). All Planet scenes were PSScene4Band (RGB, NIR) and captured using the PSB.SD PlanetScope sensor. All scenes were calibrated to surface reflectance and orthorectified with 3 m spatial resolution by Planet prior to being released. Sentinel-2 surface reflectance scenes were obtained for the six sites on dates nearest the Planet and NEON acquisition dates (Table 2). Sentinel bands two, three, four, and eight correspond to the PS blue, green, red, and NIR bands, respectively. The Sentinel scenes were reduced to these four bands and cropped to the 1 km areas for all six sites. The Sentinel scenes were maintained at their native 10 m spatial resolution. The Planet scenes were resampled to 10 m and co-aligned with the Sentinel images in order to estimate model coefficients (described below).

Table 2. Acquisition dates of images used.

Site	Planet	Sentinel	NEON
CPER	14 September 2020	13 September 2020	13 September 2020
KONZ	11 July 2020	13 July 2020	13 July 2020
NIWO	20 July 2020	20 July 2020	20 July 2020
UNDE	12 August 2020	11 August 2020	11 August 2020
WOOD	24 June 2020	24 June 2020	24 June 2020
YELL	10 July 2020	11 July 2020	11 July 2020

2.3 NEON Airborne Hyperspectral Data

The NEON Airborne Observation Platform is a light aircraft with a payload that includes an imaging spectrometer that captures reflectance in the wavelength range of 380nm to 2510nm. Bands are approximately 5nm in width, resulting in 426 individual bands. The NEON spectrometer bands corresponding to the wavelengths captured by the PSB.SD instrument were extracted from the hyperspectral images and averaged to create a reference image for the RGB, NIR bands, respectively (Table 3). The NEON hyperspectral reference images were resampled to 3 m resolution and aligned to match the Planet images.

Table 3. Planet PSB.SD wavelengths and the corresponding NEON spectrometer bands.

PSB.SD Band	PSB.SD Wavelengths (nm)	NEON Bands
Blue	465 – 515	18 – 27
Green	513 – 549	40 – 41
Red	650 – 680	55 – 60
Near Infrared (NIR)	845 – 885	94 – 101

3. METHODOLOGY

3.1 The Linear Transformation

The per-band linear transformation between a reference image and a subject image to be normalized is defined as

$$X_{trans} = a\,X_{raw} + b, \tag{1}$$

where X_{ttrans} is the transformed subject image X_{raw} is the raw subject image, and a and b are constants to be estimated[5,11]. The constants a and b can be estimated using least squares with equations provided by Jensen[5,12],

$$a = \frac{\mathrm{cov}(X,Y)}{\mathrm{cov}(X,X)} \;,\; b = \overline{Y} - a\overline{X}\,, \tag{2}$$

where Y is the reference image and X is the raw subject image.

Model coefficients were estimated using the Sentinel data as the reference image and the PS data aggregated to 10 m as the subject image (Eq. 2). Linear transformation models (Eq. 1) were then applied to the original Planet data at 3 m resolution.

3.2 Evaluation Procedure

The effectiveness of the linear transformation in matching the probability distribution of the target image to that of the reference image was assessed through the application of the Kolmogorov-Smirnov test. The Kolmogorov-Smirnov test is a nonparametric method to test the equality of probability distributions through the application of the *D* statistic and its associated p-value. The *D* statistic measures the distance between two empirical density functions under the null hypothesis that the two samples are from the same distribution. The *D* statistic ranges from 0 – 1, with lower values indicating a smaller distance and thus greater equality between the two distributions. The Kolmogorov–Smirnov test was computed per band for both the original Planet image and the transformed Planet image against the Sentinel reference image.

The absolute spectral accuracy of the transformed Planet images was evaluated against the NEON airborne hyperspectral data. The per-pixel absolute error per band was computed for both the original Planet scene and the transformed Planet scene with respect to the reference Sentinel scene.

4. RESULTS AND DISCUSSION

4.1 Comparison of Planet Relative to Sentinel

The results of the Kolmogorov–Smirnov tests of the difference between the Planet and Sentinel distributions show that *D* statistic values were as high as 0.94 (NIR band, CPER site) for the original (untransformed) data. Recall that *D* statistic values closer to 1 indicate the distributions are more dissimilar. Values near 0 indicate the distributions are similar. Values for the untransformed data ranged [0.046, 0.941] with a mean of 0.356 and a median of 0.297. In all cases, the *D* statistics comparing the untransformed Planet data to the Sentinel reference were significant ($P < 0.001$).

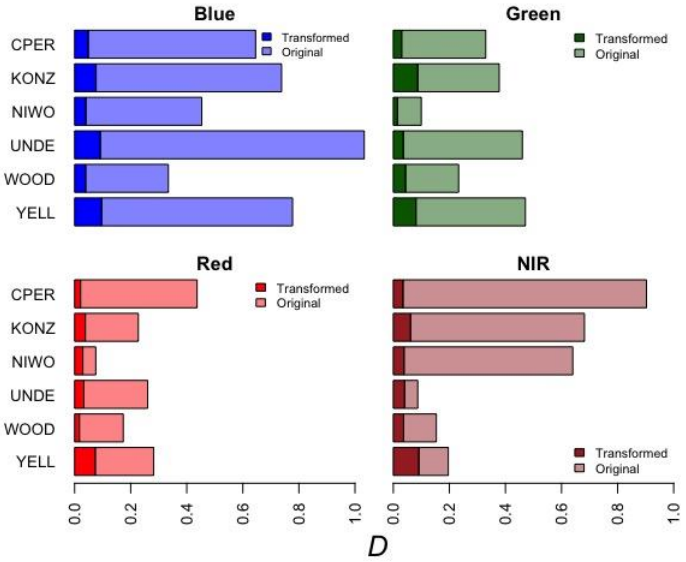

Figure 2. The Kolmogorov–Smirnov test *D* statistic comparing the original and transformed Planet data for each band for each of the six study sites. In both cases, the distribution was compared against the Sentinel distribution.

Overall, the blue and NIR bands showed greater differences between the untransformed Planet and Sentinel images than the green and red bands, particularly for the CPER, KONZ, and NIWO sites. These three sites are located at lower latitudes than the UNDE, WOOD, and YELL sites, which may be impacting the atmospheric correction procedure done internally by Planet that involves using a 6SV2.1 radiative transfer code and MODIS NRT data. The CPER, KONZ, and NIWO sites also have generally different land cover makeup than the other three sites, with higher proportions of grassland and bare ground (Fig. 1). The UNDE and WOOD sites, which both presented larger *D* statistic values for the untransformed blue and green bands compared to red and NIR, have a greater proportion of water than the other sites. While it is not possible to definitively attribute the differences to either latitude or land cover, our findings show that the

differences between the untransformed Planet reflectance and the Sentinel reference were not universally consistent across sites.

After performing the linear transformation, the *D* statistic decreased substantially for all sites and bands (Fig. 2), indicating that the linear transformation was successful in making the Planet values more similar to the Sentinel reference values. All *D* values were less than 0.1, [0.014, 0.096] with a mean of 0.045 and a median of 0.038, but the magnitude of change varied by band and site. The lowest values were observed for the red and NIR bands at all sites except YELL. Changes in values after the transformation were more variable for the blue and green bands (Fig. 2).

Ultimately, we found that the linear transformation collapsed variation effectively across all sites and bands. Despite differences between the original Planet and Sentinel values, post-transformation *D* statistic values were similar across all study sites and spectral bands. The initial differences between Planet and Sentinel reflectance values as measured through the *D* statistic does not appear to affect the linear transformation. However, despite the changes, all differences were significant ($P < 0.01$) indicating that the empirical distribution functions (ECDF) remained significantly different even after the transformation. A simple linear transformation is not likely to result in a perfect alignment of the ECDFs due to the scale mismatch between Planet and Sentinel. The upsampling of Planet to match the spatial resolution to that of Sentinel can result in a decrease in the dynamic range of pixel values, particularly in heterogeneous areas[3].

4.2 Comparison with Airborne Hyperspectral

Linear transformations such as the ones completed above do not necessarily improve the signal to noise ratio or correct radiometric errors. Rather, they only normalize the radiometric values to a reference dataset. To measure how closely the Planet reflectance values matched a ground reference standard, both before and after the transformation, we compared the values to NEON hyperspectral ground reference data described above. The linear transformations generally improved the radiometric quality of the Planet data toward the NEON reference (Fig. 3). The violin plots display the kernel density of the per-pixel error between the original Planet (lighter shade) and transformed Planet (darker shade) values vs. the NEON airborne hyperspectral data. After the transformation, the density histograms are more closely centered on the 0 line. This pattern is most clearly evident in the NIR values for the CPER site. While accuracy generally improved, there were instances where the linear transformation created larger differences between Planet and the NEON reference. Examples include the transformed green and red bands for CPER and YELL.

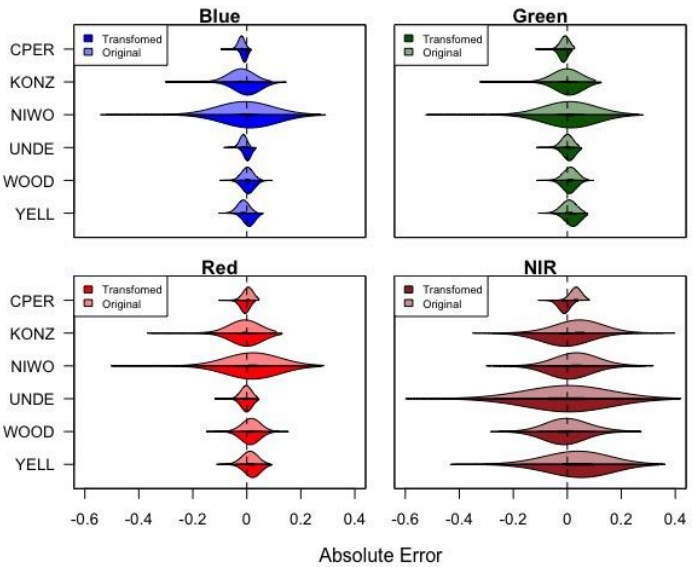

Figure 3. Violin plots per band for each of the six study sites showing absolute error of the Planet data compared to the NEON ground reference. Each side of the violin is a kernel density plot of the errors of the transformed and original Planet images.

CONCLUSION

Commercial smallsats are rapidly becoming a key resource for Earth observation, allowing for imaging at very high spatial and temporal resolutions. However, the multi-sensor constellations, combined with the low cost inherent to the sensors, results in radiometric inconsistencies that are particularly apparent when constructing a mosaic or time series. Such inconsistencies can be overcome through the process of radiometric normalization using an established reference such as Sentinel or Landsat. While a number of methods for radiometric normalization are available, linear transformations are a simple and effective way of normalizing multi-sensor image scenes to a reference standard. Here, 4-band Planet images were transformed using Sentinel images as a reference at six locations with varying land cover heterogeneity. The linear transformation applied was effective in transforming the empirical cumulative distribution functions of the Planet values to be closer to that of Sentinel. The transformation achieved similar results regardless of the initial disparity between the Planet and Sentinel images. When compared to airborne hyperspectral data, the per-pixel errors of the transformed images varied across bands and locations. Since the transformation is unable to improve radiometric quality to be greater than that of the reference image, the absolute errors in the transformation images are attributed to the spectral inconsistencies between Sentinel surface reflectance data and the airborne hyperspectral data.

REFERENCES

[1] Crusan, J., and Galica, C., "NASA's CubeSat Launch Initiative: Enabling broad access to space," Acta Astronautica 157, 51–60 (2019).

[2] Houborg, R., and McCabe, M. F., "High-resolution NDVI from Planet's constellation of earth observing nano-satellites: a new data source for precision agriculture," Remote Sens 8(9), 768 (2016).

[3] Houborg, R., and McCabe, M. F., "A Cubesat enabled Spatio-Temporal Enhancement Method (CESTEM) utilizing Planet, Landsat and MODIS data," Remote Sens Environ 209, 211–226 (2018).

[4] Helmer, E. H., "Radiometric Normalization" In B. Warf (Ed), [Encyclopedia of Geography], SAGE Publications, Thousand Oaks, CA, (2010).

[5] Hong, G. and Zhang, Y., "A comparative study on radiometric normalization using high resolution satellite images," Int. J Remote Sens 29, 425–438 (2008).

[6] Canty, M. J., [Image Analysis, Classification and Change Detection in Remote Sensing: with Algorithms for ENVI/IDL], CRC/Taylor & Francis, Boca Raton, FL, 253-257 (2007).

[7] Csillik, O., Kumar, P., Mascaro, J., O'Shea, T., and Asner, G. P., "Monitoring tropical forest carbon stocks and emissions using Planet satellite data," Scientific Reports, 9(1), 1-12 (2019).

[8] Csillik, O., Kumar, P., & Asner, G. P., "Challenges in Estimating Tropical Forest Canopy Height from Planet Dove Imagery," Remote Sens, 12(7), 1160 (2020).

[9] Xu, Y., Vaughn, N. R., Knapp, D. E., Martin, R. E., Balzotti, C., Li, J., Foo, S. A., and Asner, G. P., "Coral Bleaching Detection in the Hawaiian Islands Using Spatio-Temporal Standardized Bottom Reflectance and Planet Dove Satellites," Remote Sens 12(19), 3219 (2020).

[10] Leach, N., Coops, N. C., and Obrknezev, N., "Normalization method for multi-sensor high spatial and temporal resolution satellite imagery with radiometric inconsistencies," Comput Electron Agric 164, 104893 (2019).

[11] Kimm, H., Guan, K., Jiang, C., Peng, B., Gentry, L. F., Wilkin, S. C., Wang, S., Cai, Y., Bernacchi, C. J., Peng, J., and Luo, Y., "Deriving high-spatiotemporal-resolution leaf area index for agroecosystems in the U.S. Corn Belt using Planet Labs CubeSat and STAIR fusion data," Remote Sens Environ, 239, 111615 (2020).

[12] Jensen, J. R, "Urban/Suburban Land Use Analysis," In R. N. Colwell (Ed), [Manual of Remote Sensing] American Society of Photogrammetry, Falls Church, VA, 1571-1666 (1983).